

Electronic Supplementary Information:

**Improvements of thermoelectric properties for p-type  $\text{Cu}_{1.8}\text{S}$  bulk materials  
via optimizing mechanical alloying process**

*Peng Qin<sup>1</sup>, Xin Qian<sup>2</sup>, Zhen-Hua Ge<sup>1\*</sup>, Lei Zheng<sup>2</sup>, Jing Feng<sup>1</sup> and Li-Dong Zhao<sup>2\*</sup>*

1. Faculty of Materials Science and Engineering, Kunming University of Science and Technology, Kunming, 650093, China.
2. School of Materials Science and Engineering, Beihang University, Beijing 100191, China.

Email: zge@kmust.edu.cn; zhaolidong@buaa.edu.cn

**1. Sample preparation**

Commercial high purity powders, 99.99% Cu (under 200 mesh) and 99.99% S (under 200 mesh) were used as raw materials. These powders were subjected to MA with chemical compositions of  $\text{Cu}_{1.8}\text{S}$  in a planetary ball mill (QM-4F, Nanjing University, China) at 425 rpm for 1, 3, 7, 12, 18 h in an atmosphere of mixed gas with nitrogen (95%) and hydrogen (5%). Stainless steel vessels and balls were used, and the weight ratio of ball to powder was kept at 20:1. The stainless steel balls with three different sizes were used in our work,  $\Phi 10$ ,  $\Phi 8$ ,  $\Phi 4$ , respectively. The weight of each powder sample is 5.12 g. The ball-milled powders were sintered at 723 K for 5 min in a  $\Phi 15$  graphite mold under an axial pressure of 50 MPa in a vacuum using the SPS system (Sumitomo SPS211-X, Japan). The ramp-up speed was 80 K/min and the holding time was 5 min. The sintered specimens were disk-shaped with dimensions of 15 mm×2 mm.

**2. Properties characterization**

The phase was identified with X-ray diffraction (XRD,  $\text{CuK}\alpha$ , Bruker D8, Germany). The fractographs were observed by field emission scanning electron microscope (FESEM, ZEISS,

Germany), and an energy dispersive X-ray (EDX) spectrometer to observe the composition and distribution of the elements. A Netzsch STA 449 was used for the DSC measurements with a heating/cooling rate of 20 K min<sup>-1</sup> between 323 and 773 K in N<sub>2</sub> atmosphere. Transmission electron microscopy (TEM) investigations were carried out in a FEI Tecnai F30 microscope operated at 300 kV. The thin TEM specimens were prepared by conventional methods and include cutting, grinding, dimpling, polishing, and Ar-ion milling on a liquid nitrogen cooling stage. The Seebeck coefficient and electrical resistance were measured using a Seebeck Coefficient/Electrical Resistance Measuring System (ZEM-3, Ulvac-Riko, Japan) at 323-773K in a helium atmosphere. The thermal diffusivity ( $D$ ) was measured by laser flash method (NETZSCH, LFA457, Germany). The specific heat ( $C_p$ ) was measured using a thermal analyzing apparatus (Netzsch STA 449). The density of the sample was measured by the Archimedes method. The thermal conductivity ( $\kappa$ ) was calculated from the density ( $\rho$ ), specific heat and thermal diffusivity using the relationship  $\kappa = \rho DC_p$ .

The Hall coefficients ( $R_H$ ), carrier concentration, and carrier mobility of the samples were measured at 323 K with an applied magnetic field of 2T and an electrical current of 30 mA using a physical properties measurement system (PPMS-9T, Quantum Design Inc., USA).

The uncertainty of the thermal conductivity is estimated to be within 10%, comprising uncertainties of 3 % for the thermal diffusivity ( $D$ ), 5 % for the specific heat ( $C_p$ ), and 2 % for the sample density ( $\rho$ ). The combined uncertainty for all measurements involved in the calculation of  $ZT$  is around 20%.

### 3. Calculation details

In this paper, the calculations are performed using first principle calculations based on density functional theory (DFT) which is implemented in Cambridge sequential total energy package

(CASTEP) code. The generalized gradient approximation (GGA) in Perdew-Burke-Ernzerhof (PBE) with Grimme methods for DFT-D correction is employed as the exchange–correlation energy function [1, 2]. Ultrasoft pseudo potentials (USPPs) are used to indicate the interactions between ionic core and valence electrons with the valence configurations  $3d^{10}4s^1$  for Cu and  $3s^2p^4$  for S. The crystal reciprocal-lattice and integration over the Brillouin zone were performed using the Monkhorst-Pack grid of  $3\times 3\times 3$ . The plane-wave basis set cut-off energy was selected as 500eV for all the calculations. The plane wave expansion method is applied for the optimization of the crystal structure conducted by the Broy-den-Fletcher-Goldfarb-Shanno (BFGS) algorithm. [3-5] As shown in Fig. S1, the geometry optimizations were performed on a  $2\times 2\times 2$  supercell, of the  $\text{Cu}_2\text{S}$  primitive cell. To meet the stoichiometric ratio of  $\text{Cu}_{1.8}\text{S}$  and  $\text{Cu}_{1.96}\text{S}$ , 6 and 2 Cu atoms were removed from the supercell, respectively. The convergence parameters for the geometry optimization were as follows: total energy changes during the optimization processes were finally converged to  $2\times 10^{-6}$  eV and the forces per atom were reduced to  $0.05 \text{ eV}\cdot\text{\AA}^{-1}$ .

#### References:

- 1 P. Hohenberg and W. Kohn, *Phys. Rev.* 1964, **136**, B864.
- 2 M. Segall, P. Lindan, M. Probert, C. Pickard, P. Hasnip, S. Clark, and M. Payne, *J. Phys.: Condens.Matter*.2002, **14**, 2717.
- 3 S. Grimme, *J. Comput.Chem.*2006, **27**, 1787.
- 4 X. Wang, X. Cheng, Y. Zhang, R. Li, W. Xing, P. Zhang, X.-Q. Chen, *Phys. Chem. Chem. Phys.*2014, **16**, 26974.
- 5 J.D. Head, M.C.Zerner, *Chem.Phys.Lett.*1985, **122**, 264.

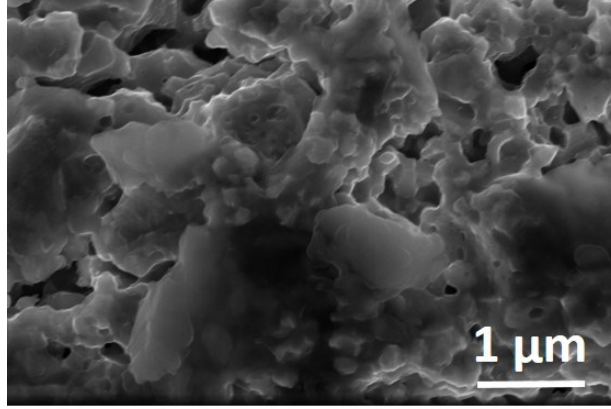


**Fig. S1:** FESEM fractograph images of  $\text{Cu}_{1.8}\text{S}$  bulk with the ball-milling time 18 h, the microstructure of the 18 h sample is very similar to that of 12 h sample.

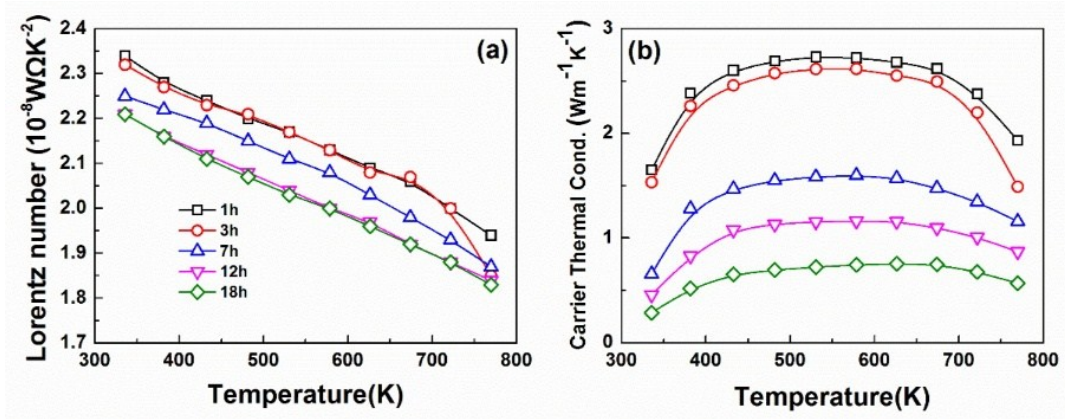


**Figure S2** the temperature dependence of Lorentz number (b) and calculated carrier thermal conductivity (c) for  $\text{Cu}_{1.8}\text{S}$  with different ball milling times for 1 h, 3 h, 7 h, 12 h, 18 h.

Reduced Fermi energy was used to calculate Lorentz number (**equ. (1)**) varies as Seebeck value changes (**equ.(2)**) with temperature or composition. The L calculation was estimated in a traditional single parabolic band model (resulting in an L with a deviation of less than 10% as compared with a more rigorous singlenon-parabolic band and multiple band models calculation) , where the reduced Fermi energy was implicitly determined by the Seebeck values (**equ.(2)**).

$$L = \left( \frac{k_B}{e} \right)^2 \left( \frac{(r + 7/2)F_{r+5/2}(\eta)}{(r + 3/2)F_{r+1/2}(\eta)} - \left[ \frac{(r + 5/2)F_{r+3/2}(\eta)}{(r + 3/2)F_{r+1/2}(\eta)} \right]^2 \right), (1)$$

$$S = \pm \frac{k_B}{e} \left[ \frac{(r + 5/2)F_{r+3/2}(\eta)}{(r + 3/2)F_{r+1/2}(\eta)} - \eta \right], (2)$$